

Background

Immunotherapy, particularly cytokine-based therapy, has been gaining traction in the treatment of head and neck cancers. Cytokines are small proteins that play a crucial role in the immune response to cancer. However, not all patients respond to cytokine-based immunotherapies, and some may experience severe side effects. The ability to predict which patients are most likely to benefit from these therapies could greatly improve the efficacy and tolerability of treatment. In this context, the study of predictive biomarkers, such as the expression of immune checkpoint molecules like PD-L1 and TIGIT, and the profiling of cytokines within the tumor microenvironment, has become crucial. These biomarkers could provide valuable information about the patient's immune response to the tumor and their likelihood of responding to cytokine-based immunotherapies.

Method

A multimodal approach to stratify predictive biomarkers in head and neck cancers was used. The methodology was founded on combining metabolic, transcriptomic, and proteomic data to offer a comprehensive understanding of potential biomarkers. Twenty-one (21) FFPE sections from retrospectively collected screening metastases H&N tumors biopsies treated with cytokine-based immunotherapy were used. Patients were classified in two groups according to their Objective Response Rate (ORR): Responder (R) and Non-Responder (NR) for spatial metabolomic and transcriptomic assays. Matrix-assisted laser desorption/ionization (MALDI-MSI) to analyze metabolic spatial distribution and GeoMx[®] DSP assay (Nanostring[®]) Whole transcriptomic assay were performed. The statistical analysis was performed through the GeoMx[®] DSP analysis suite and Multimaging[™].

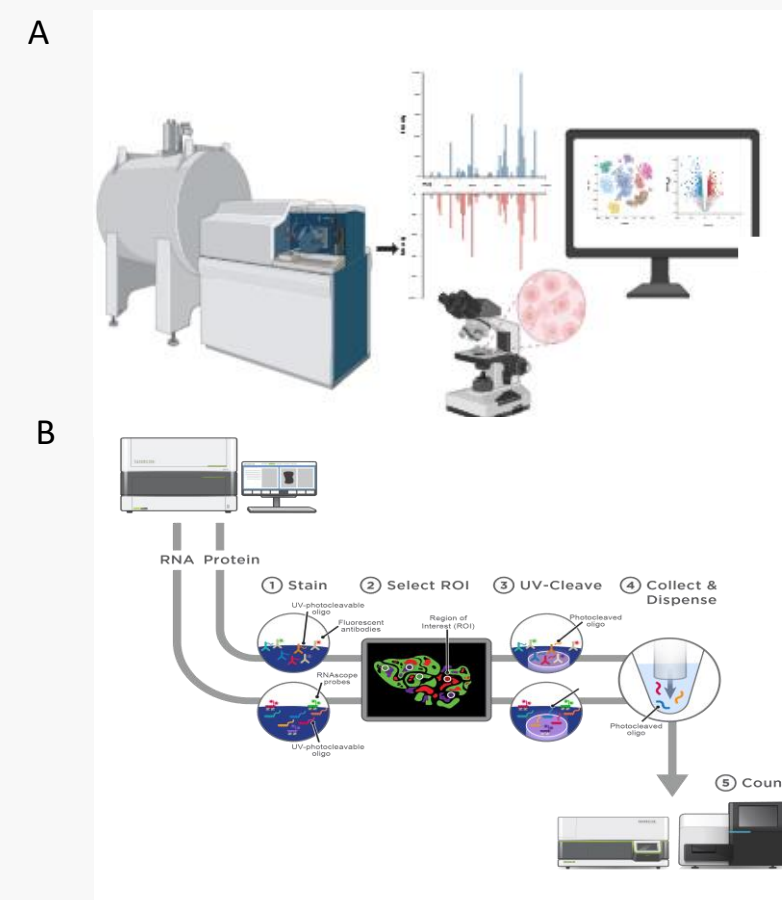


Figure 1 A- Tissue imaging was performed at high spatial resolution, in positive and negative ion mode, in full scan mode 75–1200 m/z. B-Whole Transcriptome analysis workflow.

Spatial Metabolomic Profiling

Metabolomic profiles of R and NR samples were acquired by MALDI-MSI. First, exploratory data analysis by clustering was performed to identify differences between the two responses groups (Fig. 2). Batch corrected MSI data were projected in a UMAP tri-dimensional plot, based on the spectra's peaks intensities. *K-means* clustering identified clusters by spectral or biochemical patterns similarities. However, clusters differentiating R from NR patients were not observed.

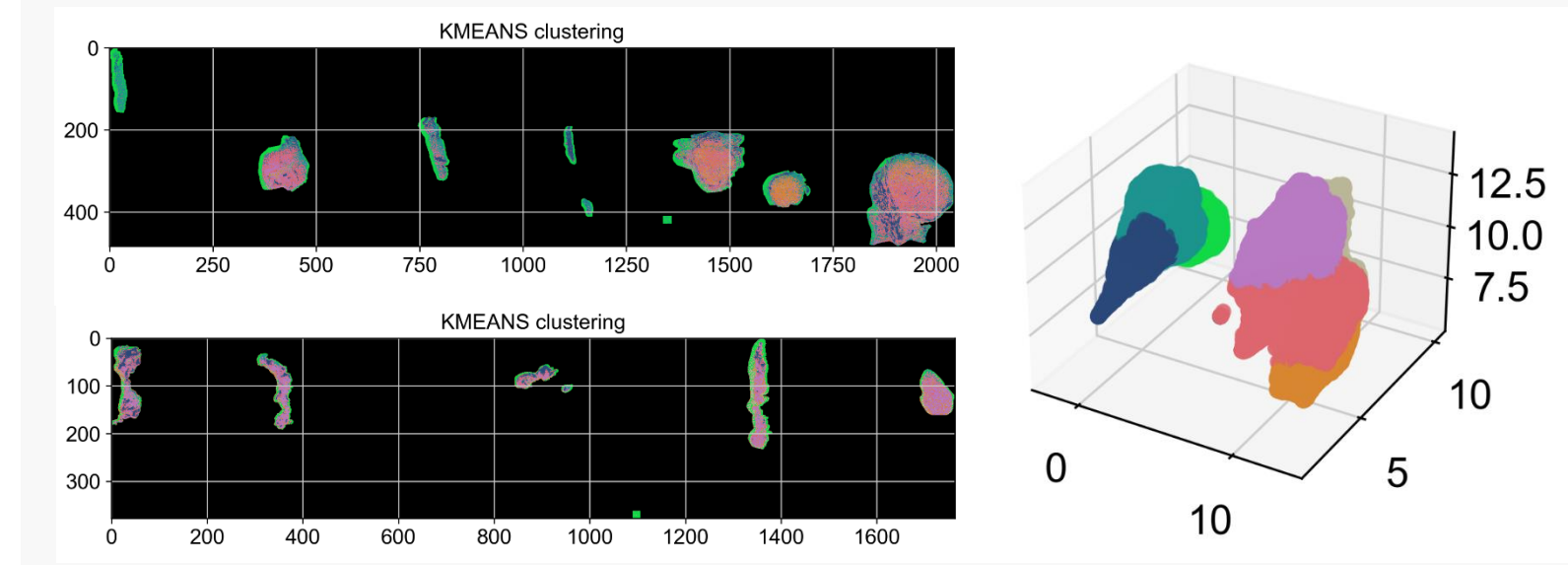


Figure 2 A-Immune cells infiltration within the tumor landscape in PD patient Left and CR patient right. Pie chart representing the relative percentage of immune cells present in the PD left and in CR tumor microenvironment right.

Statistical comparison was also performed to identify modulated features between the groups (Fig. 3). In the R group, overexpression of features were found to be statistically different. Further annotation identifies the presence of ceramides in the R cohort.

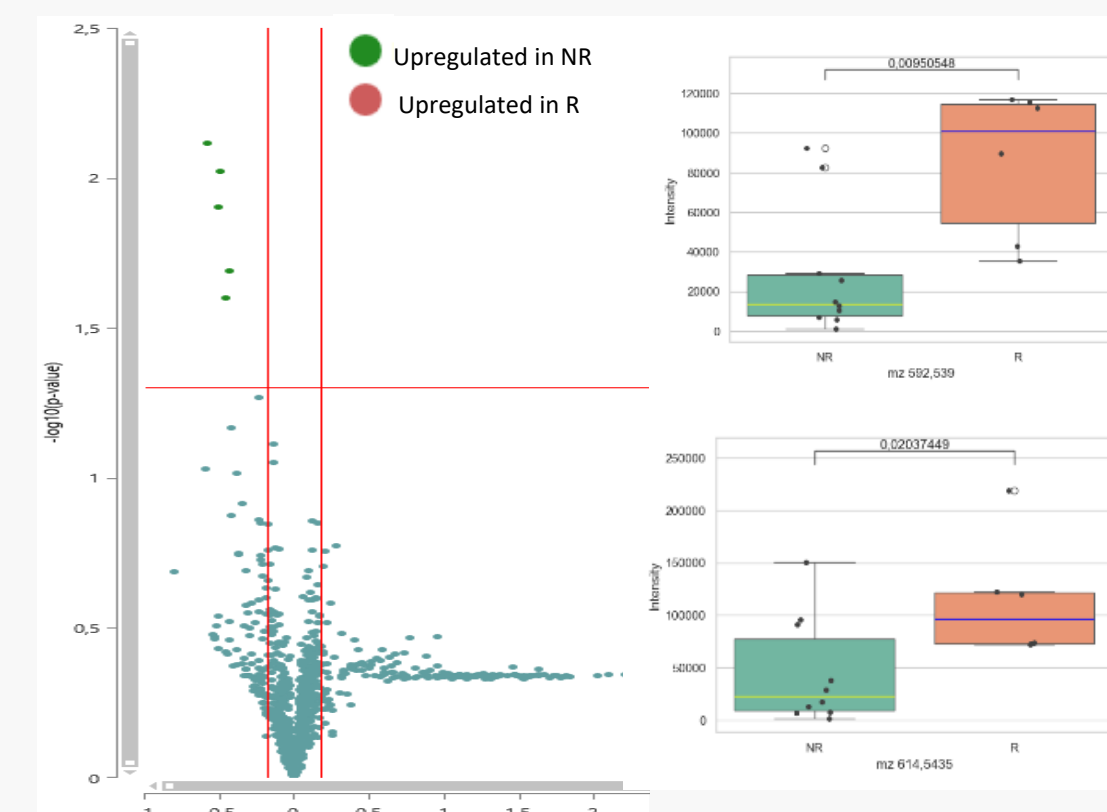


Figure 3 Volcano plot depicting differentially expressed features P value as a function of fold change between the R cohort compared to the NR response & Bar graph showing the significant overexpression of ceramides in the R group. .

Spatial Transcriptomic Profiling

6 regions of interest (ROIs) per sample were selected based on morphological staining of immune cell (CD45) and tumor cells (PanCK) (Fig. 4). Based on these fluorescent labels, Interface regions were selected that were enriched for CD45 staining, and Tumor regions enriched with PanCK were detected. Unsupervised gene expression analysis revealed a large gene expression modulation without a clear differentiation between the R and the NR cohorts.

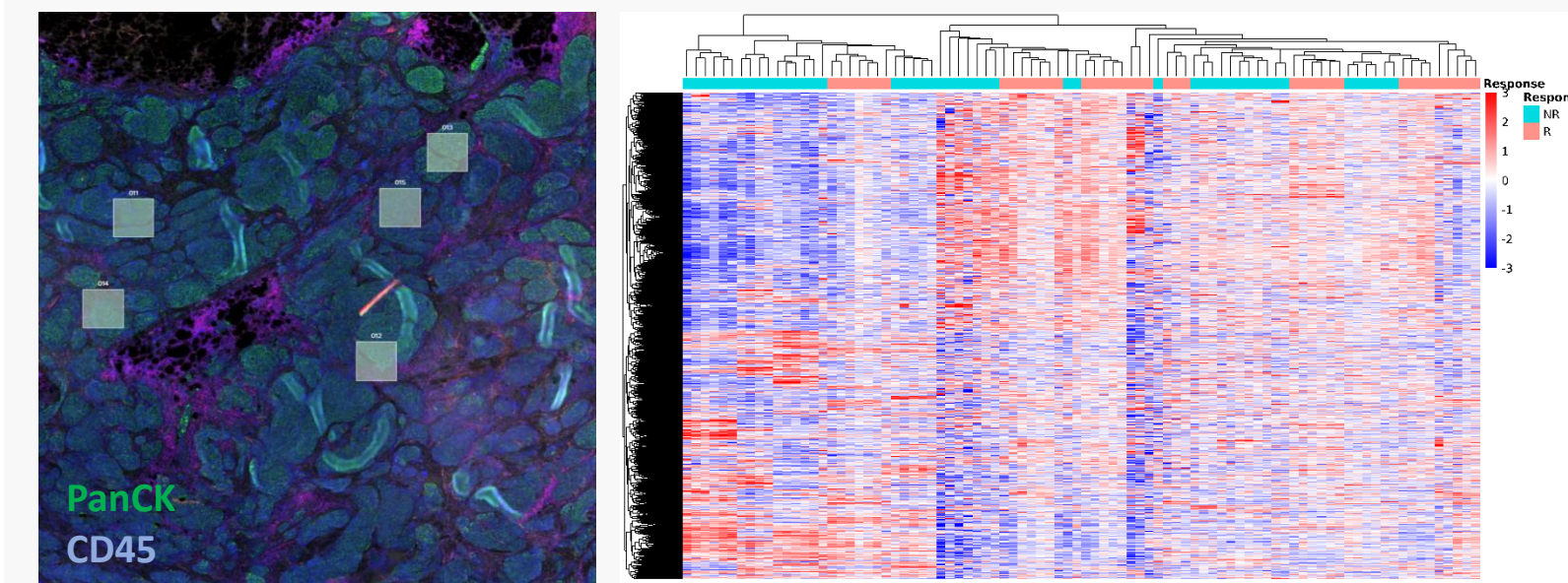


Figure 4 Selection of tumor-rich and interface rich regions within mH&E tumors stained with fluorescently labeled anti-pan-cytokeratin (green) and anti-CD45 (magenta). Representative analyzed regions of interest (ROIs) are shown. Heatmap representing the clustering of expression levels of genes in all regions.

High expression of genes related to signaling by interleukin pathways was observed in the R cohort in the tumor region (Fig. 5). Interestingly, the upregulation of gene expression in the interface in the R cohort is related to G-proteins coupled receptors signaling.

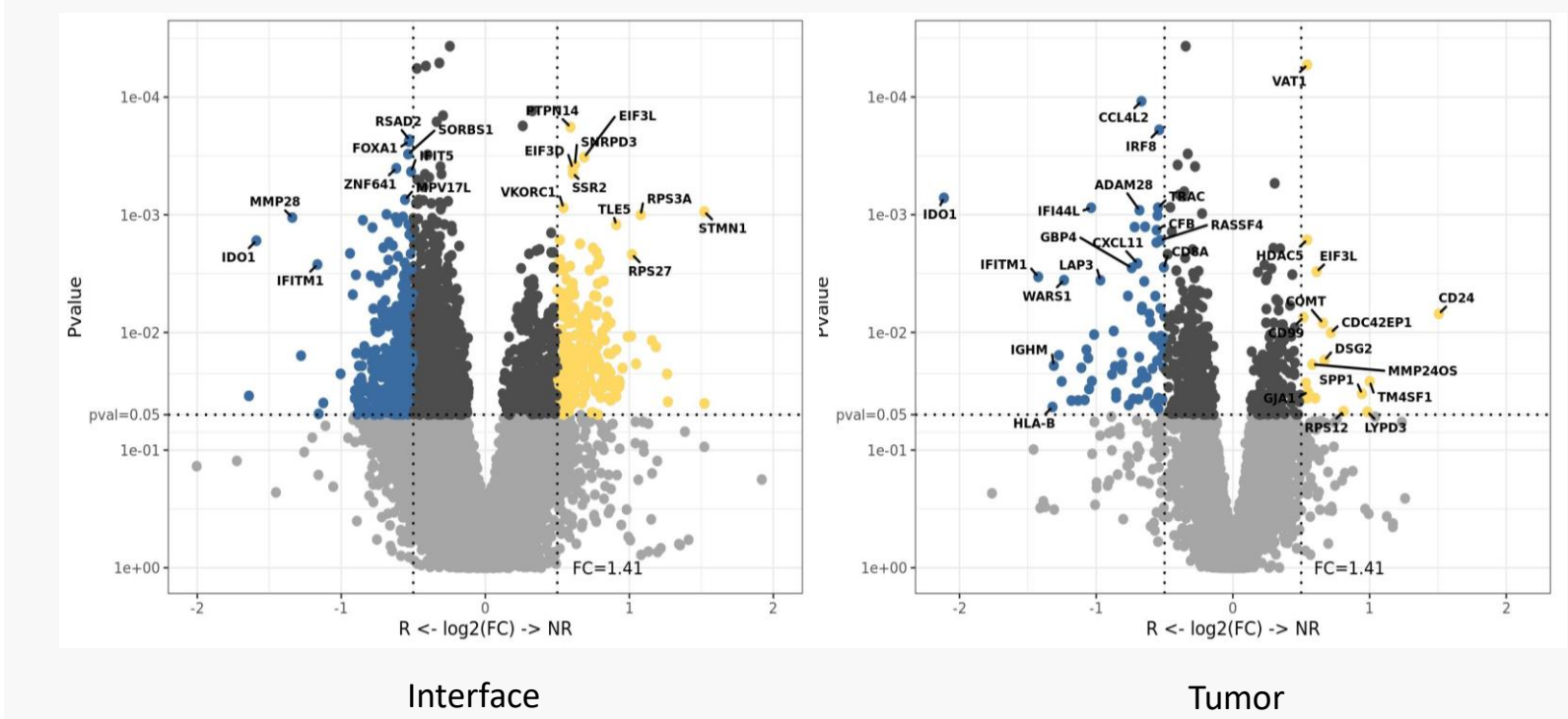


Figure 5 Volcano plots highlighting the differences in mRNAs differentially regulated in the two response cohorts within different histological compartment.

Pathways Analysis

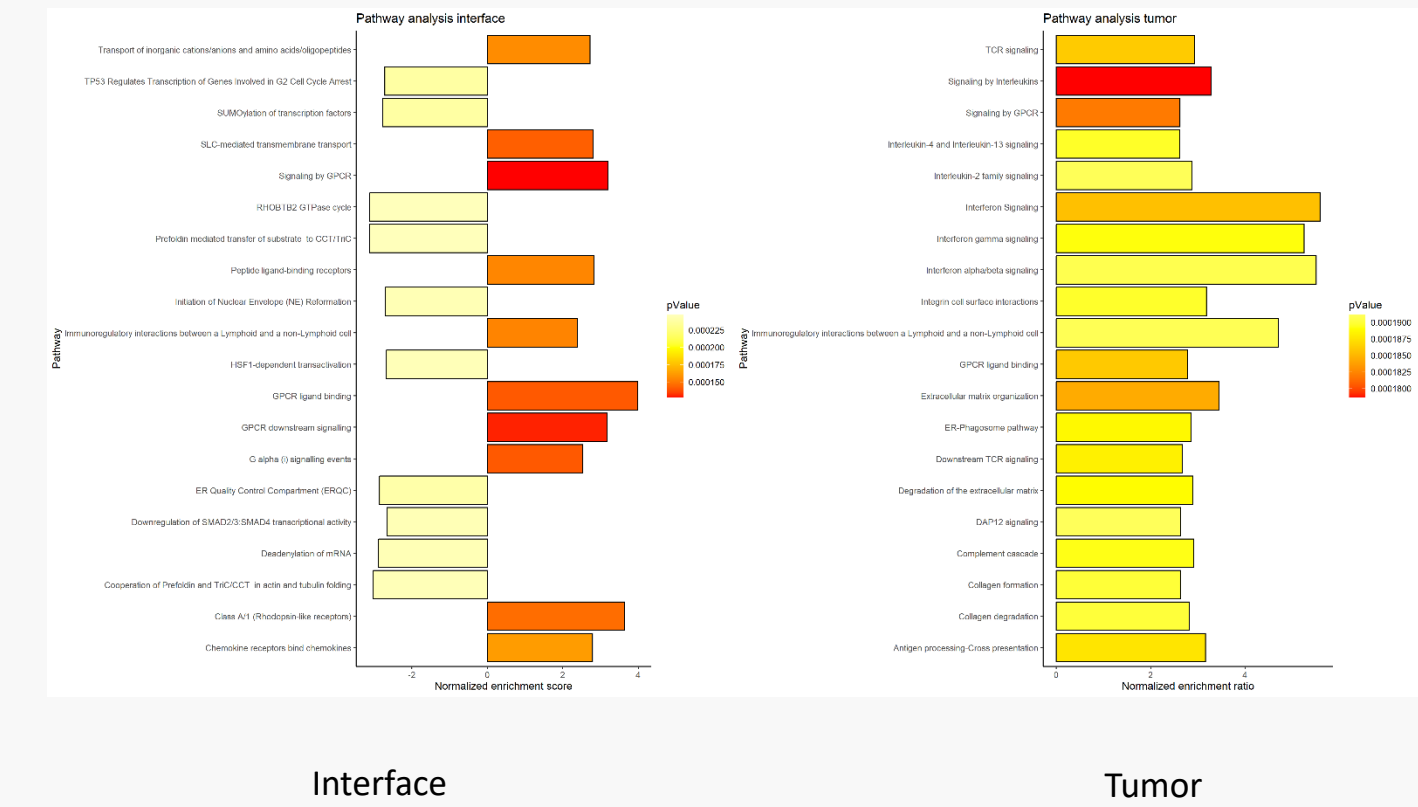


Figure 6 Enrichment score representation of the modulation of regulation of the biological pathways in Interface and Tumor regions.

Conclusion

Our study demonstrates the considerable potential of a multimodal stratification approach in deciphering the complexity of head and neck cancers and predicting responses to cytokine-based immunotherapies. By integrating metabolomic and transcriptomic data, we identified unique biomarker signatures that strongly correlated with therapy responses. This work underscores the invaluable role of integrated predictive biomarker profiles in enhancing the precision of immunotherapy.

References

- Croci DO, Zacarias Fluck MF, Rico MJ, Matar P, Rabinovich GA, Scharovsky OG. Dynamic cross-talk between tumor and immune cells in orchestrating the immunosuppressive network at the tumor microenvironment. *Cancer Immunol Immunother.* 2007;56(11):1687-1700.
- Baghban R, Roshangar L, Jahanban-Esfahlan R, et al. Tumor microenvironment complexity and therapeutic implications at a glance. *Cell Commun Signal.* 2020;18(1):59.
- Hanahan D, Coussens LM. Accessories to the crime: functions of cells recruited to the tumor microenvironment. *Cancer Cell.* 2012;21(3):309-322.
- Xu K, Rahmatpanah F, Jia Z. Editorial: Therapeutic Opportunities and Innovative Biomarkers in Tumor Microenvironment. *Front Oncol.* 2021;11:803414.